

# Prediction of Steady State Dispersion Height from Batch Settling Data

In order to design continuous industrial settlers, it has in the past been necessary to obtain extensive pilot plant data, the interpretation of which required considerable experience before it could be used for scale-up purposes. The idea of using batch settling tests has always seemed attractive, but the difficulty of reconciling unsteady- and steady-state experiments has so far proved physically and mathematically insurmountable.

In this study the variation in steady state height with dispersion throughput in a continuous settler is predicted from unsteady state data obtained in a small-scale batch settler. Models are presented which relate the drop sedimentation and coalescence in batch and continuous dispersions, thus enabling the steady state settler behavior to be predicted from parameters obtained from the batch data. These models are verified with available experimental data and should greatly simplify the future design and scale-up of continuous settlers.

S. A. K. JEELANI and  
STANLEY HARTLAND

Department of Chemical Engineering and  
Industrial Chemistry  
Swiss Federal Institute of Technology  
8092 Zurich, Switzerland

## SCOPE

Although the coalescence of liquid drops is important in many industrial operations, particularly in gravity settlers, the behavior of liquid-liquid dispersions and the coalescence process is only qualitatively understood. This is probably due to the presence of indeterminate amounts of surface-active agents, thus making reproducible data very difficult to obtain. Only empirical equations exist which relate the steady state dispersion height to the dispersion throughput. The unknown parameters they contain can in principle be extrapolated from costly pilot plant experiments. However, in practice this is usually not possible because of the difficulty of matching op-

erating conditions, such as drop size distribution and the degree of turbulence.

The object of the present study is to show how the relevant parameters can be obtained from batch-settling experiments and successfully used to predict the variation in steady state height with dispersion throughput. Physical models based on drop sedimentation and coalescence are presented which apply to both batch and continuous dispersions. The constants involved can thus be derived from small-scale batch experiments and used to predict the variation in steady state height with throughput on a larger scale.

## CONCLUSIONS AND SIGNIFICANCE

Models have been obtained which relate the behavior of batch and continuous dispersions. These enable the variation in steady state dispersion height with throughput to be predicted from parameters measured in batch experiments.

The decay in batch dispersion height  $h$  with time  $t$  is usually exponential but may possess an inflection point if the initial rates of sedimentation and coalescence are slow. The exponential decay data of Vieler (1977) can be represented by the reciprocal relationship:

$$\frac{1}{-dh/dt} = \frac{1}{k_1} \frac{1}{h} + \frac{1}{k_2} \quad (i)$$

which corresponds to the variation in steady state height  $H$  with dispersion flux  $Q/A$ :

$$\frac{1}{Q/A} = \frac{1}{k_1} \frac{1}{H} + \frac{1}{k_2} \quad (ii)$$

proposed by Stönnner and Wöhler (1975). The constants  $k_1$  and  $k_2$  can thus be obtained from batch decay data and used to predict the steady state behavior if the drop size, turbulence, coalescence rates and of course the degree of contamination are similar to both batch and continuous experiments.

The sigmoidal decay curves of Barnea and Mizrahi (1975d) reflect the inflection points in the sedimenting and coalescing

fronts expressed as distances  $x$  and  $y$  measured from the final undisturbed interface (so that  $x + y = h$ ). Allowing for drop growth by binary coalescence, the initial increase in sedimentation rate  $-dx/dt$  relative to the static continuous phase with time  $t$  is given by:

$$-\frac{dx}{dt} = 0.054 t^{0.42} \quad (iii)$$

in cgs units. The sedimenting drops collect at the disengaging interface to form a dense-packed layer of height  $h_p$  which initially increases in thickness, since the volume rate of sedimentation is greater than the volume rate at which the drops coalesce with their homophase. Allowing for the effect on the rate of coalescence of the weight of the drops pressing on the disengaging interface leads to:

$$\bar{\epsilon}_p h_p = 355 \left( \frac{-dy}{dt} \right)^{2.91} \quad (iv)$$

in cgs units. The holdup fractions in the sedimentation and dense-packed zones are  $\bar{\epsilon}_s$  and  $\bar{\epsilon}_p$  and the total batch height  $h = h_s + h_p$ .

The steady state equivalent of the sedimentation velocity  $-dx/dt$  is the velocity of the dispersed phase,  $Q_d/A\bar{\epsilon}_s$ . The elapsed time  $t$  in which the drops grow is equivalent to the

residence time  $\bar{\epsilon}_s H_s A / Q_d$ . So the steady state equivalent of Eq. iii is:

$$H_s = 1.043(Q_d / A \bar{\epsilon}_s)^{3.4} \quad (\text{v})$$

The volume rate of coalescence  $-dy/dt$  is directly equivalent to  $Q_d/A$ , so that Eq. iv becomes:

$$\bar{\epsilon}_p H_p = 355(Q_d / A)^{2.91} \quad (\text{vi})$$

Adding  $H_s$  and  $H_p$  gives the steady state dispersion height,  $H$ , if the hold-ups  $\bar{\epsilon}_s$  and  $\bar{\epsilon}_p$  in the batch and continuous experiments are identical, which may not be so if turbulence conditions differ.

It is also possible to empirically relate the batch separation time  $t_f$  corresponding to a standardized initial height  $h_o$  to the dispersion throughput  $Q/A$  producing a given steady-state height,  $H$ . We have generalized this relationship and found that

for the data of Barnea and Mizrahi (1975d)  $H$  is in fact given by Eq. ii, expressed in cgs units for their phase system A where

$$1/k_1 = 0.1543 t_f + 8.0; \quad 1/k_2 = 0.0204 t_f + 0.03825 \quad (\text{vii})$$

for water-in-oil dispersion and

$$1/k_1 = 0.3415 t_f - 8.7; \quad 1/k_2 = 0.01154 t_f + 0.4497 \quad (\text{viii})$$

for oil-in-water dispersion.

It must be emphasized that the empirical constants in Eqs. vii and viii are functions of the phase system and operating conditions used. The work involved in determining these constants for other systems is far greater than that required by the models described above, which relate the batch decay and steady state behavior of dispersions. These models have been verified with available experimental data and should greatly simplify the future design and scale-up of continuous settlers.

## INTRODUCTION

The design of industrial gravity settlers is usually based on data from pilot plant mixer-settlers involving high capital cost and a large solvent inventory which necessitates elaborate cleaning procedures to minimize the contamination of liquids. For this reason the possibility of designing large continuous settlers on the basis of small-scale batch settling tests has been considered, but in practice only a few of the attempts made have met with even limited success. This is due to the complexity of the separation mechanism which furthermore differs in the batch and steady-state processes.

The degree of complexity involved in the separation mechanism of liquid-liquid dispersions is apparent from the experimental investigations of Barnea and Mizrahi (1975a,b,c,d) who proposed only an empirical relation between the batch separation time and nominal settler capacity per unit area of the continuous settler. Extending the idea of using the batch separation time, Golob and Modic (1977) empirically correlated the batch coalescence rate of the dispersed phase in the time interval where it is approximately constant with the physical properties for a number of solvent systems with water as one of the phases. Godfrey et al. (1979) suggested a graphical interpretation of batch settling curves to predict the continuous settler performance. Stönnner and Wöhler (1975) related the continuous settler throughput per unit area to the steady state dispersion thickness based on an analogy with two-stage successive chemical reaction. Their results were experimentally verified by Vieler et al. (1979).

In the present paper models are formulated which are based on binary coalescence between drops and coalescence at the disengaging interface and which involve neither the analogy with a chemical reaction nor empirical relationships; drop sedimentation may also be allowed for. Equations are derived which relate the behavior of batch and continuous dispersions, thus enabling the variation in steady state height with dispersion throughput to be predicted from batch settling data. In addition, the steady state height is empirically related to the dispersion throughput in terms of batch separation time. However, constants are involved which must be independently determined for each liquid-liquid system and set of operating conditions used. The physical models presented are verified by experimental data available in the literature and should greatly simplify the scale-up of mixer settlers.

## Behavior of Dispersions

When a liquid-liquid dispersion is introduced into a settler the thickness of the dispersion band increases with time until a steady state is attained. The steady state dispersion height  $H$  increases with dispersion throughput  $Q/A$  until the flooding point is reached, as

shown in Figure 1b. The variation can be expressed by the reciprocal relationship (Stönnner and Wöhler, 1975):

$$\frac{1}{Q/A} = \frac{1}{k_1} \cdot \frac{1}{H} + \frac{1}{k_2} \quad (\text{1a})$$

where  $k_1$  and  $k_2$  are constants and  $A$  the cross-sectional area of the dispersion. Over a limited range below the flooding point the power law relationship

$$H = K(Q/A)^w \quad (\text{1b})$$

in which  $K$  and  $w$  are constants, is often used. However, Barnea and Mizrahi (1975d) pointed out that for both oil-in-water (o/w) and water-in-oil (w/o) type dispersions, the data of Ryon et al. (1959, 1960, 1963) could be expressed in the form

$$H = 2457 (Q_d/A)^{2.1}$$

where  $Q_d = \epsilon_F Q$  is the dispersed phase throughput which is plotted on logarithmic coordinates in Figure 1a, the constants being obtained from a least square fit. The dispersed phase throughput  $Q_d = \epsilon_F Q$ , where  $\epsilon_F$  is the feed holdup fraction of the dispersed phase

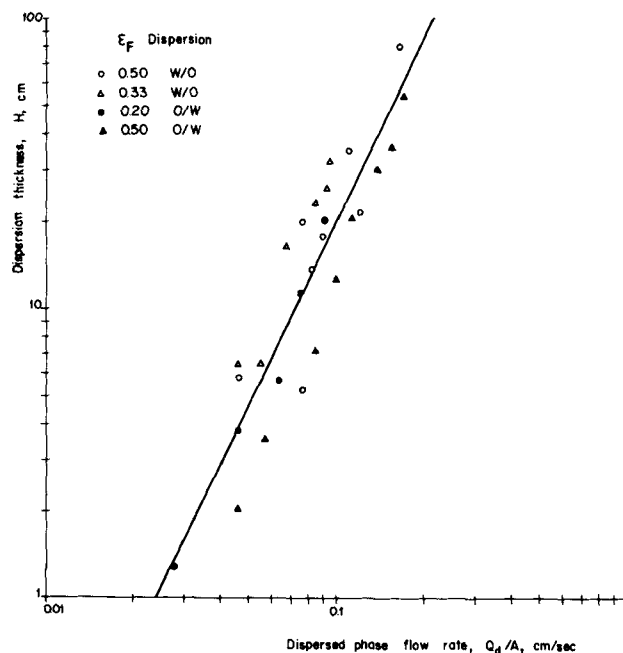


Figure 1a. Experimental variation of steady state height  $H$  with dispersed phase throughput  $Q_d/A$  on logarithmic coordinates; data of Ryon et al. (1959).

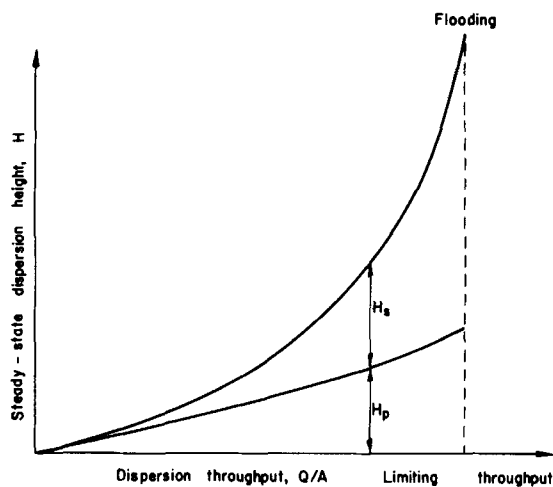


Figure 1b. Schematic variation in steady state height  $H$  with dispersion throughput  $Q/A$  showing flooding point and heights  $H_s$  and  $H_p$  of sedimentation and dense-packed zones.

which depends on the feed flow ratio to the settler.

At the steady state the drops grow in size by binary coalescence and sediment to form a dense-packed layer adjacent to the disengaging interface where the drops coalesce with their homophase. The total dispersion height  $H$  is the sum of the sedimentation and dense-packed heights  $H_s$  and  $H_p$ , as shown in Figure 1b.

If the feed rate is reduced to zero the dispersion decays in a time  $t_f$  as the sedimentation and coalescence processes continue, as shown in Figure 2. Batch dispersions can also be directly sampled from the process stream or formed independently in a small-scale mixing vessel. The total batch dispersion height  $h$  is the sum of the heights  $h_s$  and  $h_p$  of the sedimenting and dense-packed zones. It is also equal to the sum of the distances  $x$  and  $y$  of the sedimenting and coalescing fronts measured from the final undisturbed interface. The heights  $x$ ,  $y$ , and  $h$  invariably decrease with time, but  $h_p$  may initially increase if the sedimentation rate is higher than the coalescence rate, as illustrated in Figure 2. This may give rise to inflection points in the variation of  $y$  and  $h$  with time  $t$ , as shown in Figures 2 and 3a. Alternatively, the decay may be exponential, Figure 3b. It is the aim of this paper to predict the variation of steady state dispersion height  $H$  with throughput  $Q/A$  from the

decay of batch dispersion height  $h$  with time  $t$  or from the individual variations of the sedimenting and coalescing fronts  $x$  and  $y$ .

## THEORETICAL

### Binary Coalescence

Consider a volume  $V$  of a liquid-liquid dispersion in which at time  $t$  there are  $N$  drops of diameter  $\phi$  and the dispersed phase holdup is  $\epsilon$ . Although  $V$  and  $\epsilon$  may change with time, the volume of the dispersed phase  $V\epsilon = N\pi\phi^3/6$  remains constant, so differentiating with respect to time yields

$$-\frac{1}{N} \frac{dN}{dt} = \frac{3}{\phi} \frac{d\phi}{dt} \quad (2)$$

If the instantaneous binary coalescence time is  $\tau_b$ , the fraction of drops coalescing in a differential time interval  $\delta t$  is  $\delta t/\tau_b$  so the number of drops coalescing will be  $N\delta t/\tau_b$ , which will reduce the total number by  $N\delta t/2\tau_b$ . Equating this to the product of the differential time interval  $\delta t$  and the rate of reduction in number of drops  $-dN/dt$  thus leads to

$$-\frac{dN}{dt} = \frac{N}{2\tau_b} \quad (3)$$

which is of course analogous to the equation governing a first-order chemical reaction with variable rate constant  $1/(2\tau_b)$ . Combining Eqs. 2 and 3 gives the rate of increase in drop diameter as

$$\frac{d\phi}{dt} = \frac{\phi}{6\tau_b} \quad (4)$$

in which  $\tau_b$  is in general a function of time and will vary with the drop size, so that

$$\tau_b = \tau_{b*} \left( \frac{\phi}{\phi_*} \right)^n \quad (5)$$

where  $\tau_{b*}$  is the binary coalescence time for drops of reference diameter  $\phi_*$ . Setting this in Eq. 4 and integrating with  $\phi = \phi_o$  when  $t = 0$  gives

$$\frac{\phi}{\phi_o} = \left( 1 + \frac{t}{t_o} \right)^{1/n} \quad (6a)$$

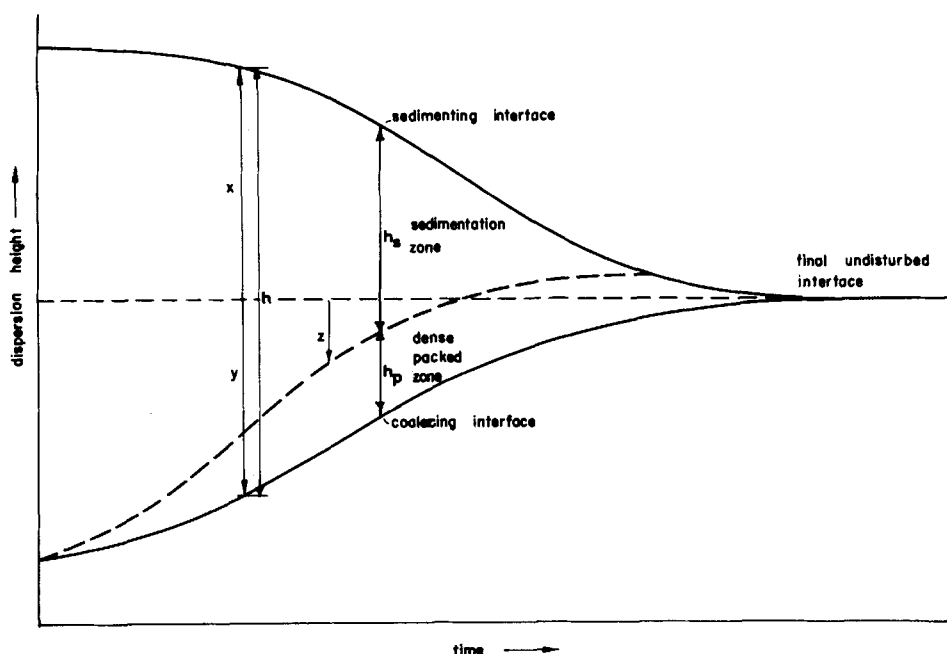


Figure 2. Schematic variation in heights  $x$  and  $y$  of sedimenting and coalescing interfaces relative to final undisturbed interface for batch dispersion. (Also shown: variation in sedimentation and dense-packed heights  $h_s$  and  $h_p$  with time  $t$ .)

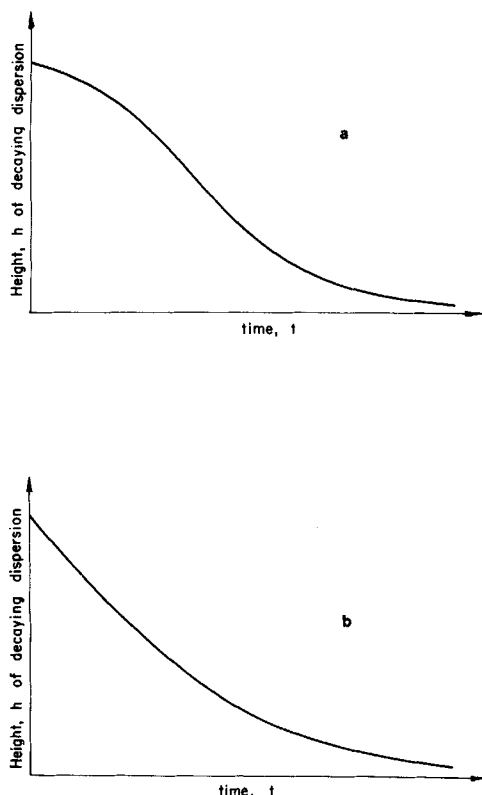


Figure 3. Schematic illustrations: (a) sigmoidal decay of batch dispersion height  $h$  with time  $t$ ; (b) exponential decay of batch dispersion height  $h$  with time  $t$ .

in which  $t_o = (\phi_o/\phi_*)^n 6\tau_{b*}/n$  is the time needed for drops to grow in size from zero to  $\phi_o$ . Should the reference condition be so chosen that  $\phi_* = \phi_o$  and  $\tau_{b*} = \tau_{bo}$ , then  $t_o = 6\tau_{bo}/n$ , where  $\tau_{bo}$  is the initial binary coalescence time. In any case Eq. 6a reduces to

$$\frac{\phi}{\phi_o} = \left(\frac{t}{t_o}\right)^{1/n} \quad (6b)$$

when  $t \gg t_o$ . Barnea and Mizrahi (1975c) did in fact find experimentally that the drop size  $\phi$  grew as  $t^{1/n}$ . These equations can be used to express the growth of the drop size,  $\phi$  with elapsed time  $t$  in batch dispersions and with drop residence time  $t$  in continuous steady state dispersions.

### Coalescence at the Disengaging Interface

The drops enter the dense-packed dispersion after having grown in size by binary coalescence during their settling process: at the disengaging interface the drops coalesce with their bulk homophase. If  $\epsilon_i$  is the dispersed phase hold-up fraction at the disengaging interface, then in an area  $A$  there are thus  $4A\epsilon_i\gamma_i/\pi\phi_i^2$  drops of mean diameter  $\phi_i$  if  $\gamma_i$  is a shape factor which allows for their nonsphericity, which is less than unity when the drop is flattened, as is the usual case. The number of drops coalescing in unit time is thus  $4A\epsilon_i\gamma_i/\pi\phi_i^2\tau_i$ , where  $\tau_i$  is the average time for each drop to coalesce with its homophase. Since the mean drop volume is  $\pi\phi_i^3/6$  the volume rate of coalescence per unit area  $\psi_i$  is thus given by

$$\psi_i = 2\gamma_i\epsilon_i\phi_i/3\tau_i \quad (7)$$

In a decaying batch dispersion of height  $h$  and mean holdup  $\bar{\epsilon}$ , the volume rate of coalescence at the disengaging interface is equal to the rate of decrease in dispersion volume  $-d(\bar{\epsilon}h)/dt$ , and in a continuous settler operating at the steady state  $\psi_i$  is equal to the volume throughput of dispersed phase per unit area  $Q_d/A$ .

Since in a dense-packed dispersion  $\gamma_i$  and  $\epsilon_i$  are constant and close to unity, the volume rate of coalescence is effectively deter-

mined by the ratio  $\phi_i/\tau_i$ . The value of  $\phi_i$  depends on the degree of binary coalescence which has occurred before the drops reach the coalescing interface, and  $\tau_i$  depends on how it is affected by  $\phi_i$  and the magnitude of the gravitational forces pressing on the draining film. The gravitational forces depend on the depth of the dense-packed layer which, in turn, we will assume to depend on the dispersion thickness. Thus,  $\tau_i$  can be expressed as

$$\tau_i = \tau_{i*} \left(\frac{\phi_i}{\phi_*}\right)^m / f\left(\frac{\epsilon h}{\epsilon_* h_*}\right) \quad (8)$$

where  $\tau_{i*}$  is the coalescence time at the coalescing interface when the drop diameter is  $\phi_*$  and the product of dispersion height and hold-up is  $\epsilon_* h_*$ . Lawson (1967) and Davies et al. (1971) reported that the experimental coalescence time of a single droplet on a flat interface to be proportional to  $\phi^m$ .

Combining Eqs. 6b, 7, and 8 gives:

$$\psi_i = \frac{2\gamma_i\epsilon_i\phi_*^m}{3\tau_{i*}} \phi_o^{1-m} \left(\frac{n}{6\tau_{bo}}\right)^{(1-m)/n} t_i^{(1-m)/n} f\left(\frac{\epsilon h}{\epsilon_* h_*}\right) \quad (9)$$

in which  $t_i$  is the time needed for the drops to reach the coalescing interface of a batch or a continuous dispersion. In a batch dispersion  $t_i$  is the elapsed time and in a continuous dispersion the drop residence time in the sedimenting and dense-packed zones.

In a batch decaying dispersion the drops sediment and begin to form a dense-packed bed of drops which coalesce at the disengaging interface. The thickness of this dense-packed layer increases with time if the rate of drop sedimentation exceeds the rate of coalescence at the interface, decreasing again when sedimentation is complete. The occurrence of a maximum in dense-packed layer thickness is reflected by the inflection point in the coalescence fronts of Barnea and Mizrahi (1975a,d). On the other hand, there are certain other types of data (Vieler et al., 1977) in which no inflection point occurs in the batch decay curve. For both types of data the function  $f(\epsilon h/\epsilon_* h_*)$  can be represented by

$$f\left(\frac{\epsilon h}{\epsilon_* h_*}\right) = \frac{c_1(\epsilon h/\epsilon_* h_*)^p}{1 + c_2(\epsilon h/\epsilon_* h_*)^q} \quad (10)$$

in which  $c_1$  and  $c_2$  are constants. This passes through a maximum at

$$\frac{\epsilon h}{\epsilon_* h_*} = \left\{ \frac{p}{c_2(q-p)} \right\}^{1/q} \quad (11)$$

giving rise to inflection points in the variations of  $h$  and  $y$  with  $t$ . The equation reduces to simpler forms, in particular when  $p = q = 0$ ,  $f(\epsilon h/\epsilon_* h_*)$  is a constant independent of  $\epsilon h$  and when  $q = 0$  is a direct power function of  $\epsilon h$ . However, the most important special case occurs when  $p = q = 1$ . The maximum in  $\epsilon h/\epsilon_* h_*$  is then infinite so inflection points do not occur and the batch decay curves are exponential in form.

### PREDICTION

The variation in steady state height with dispersion throughput can be predicted from batch decay curves. As explained in the Introduction, these are either exponential or sigmoidal in form, so both cases are considered as discussed below.

### Exponential Batch Decay

For single drops, values of  $m$  ranging from less than zero to greater than one have been reported in the literature (Burrill and Woods, 1973; Charles and Mason, 1960; Komasa and Otake, 1970; Lawson, 1967), the value being affected by the presence of surface-active agents. However, the most common value lies in the region of unity (Jeffreys and Hawksley, 1965; Hanson and Brown, 1967). For dense-packed dispersions we will assume that  $\tau_i$  is proportional to  $\phi_i$  so that  $m = 1$  when the relevant form of Eq. 9 reduces to

$$\psi_i = \frac{2\gamma_i\epsilon_i\phi_*}{3\tau_{i*}} \frac{c_1(\epsilon h/\epsilon_* h_*)}{1 + c_2(\epsilon h/\epsilon_* h_*)} \quad (12)$$

TABLE 1. CONDITIONS FOR STEADY STATE RUNS  
Data of Vieler et al., 1979

Run No.	Water Flow Rate L/s	Kerosene Flow Rate L/s	Mixer Speed rpm
1	2.30	2.55	200
2	2.50	2.93	200
3	2.13	2.30	200
4	1.12	1.44	240
5	1.63	1.00	250
6	1.12	1.00	225

which implies that the volume rate of coalescence is independent of the drop size at the disengaging interface. (Subsequent analysis of the available experimental data for coalescence in batch and continuous dispersions confirms that this is in fact the case).

Equation 12 may be expressed in the form

$$\frac{h}{-dh/dt} = \frac{1}{k_1} + \frac{1}{k_2} h \quad (13a)$$

where  $k_1 = 2\gamma_i \epsilon_i \phi_* c_1 / 3\tau_i \epsilon_* h_*$  and  $k_2 = 2\gamma_i \epsilon_i \phi_* c_1 / 3\tau_i \bar{\epsilon} c_2$  if it is assumed that  $\epsilon = \bar{\epsilon}$  is independent of time.

If the mechanism of coalescence is the same in batch and continuous settling,  $h$  and  $(-dh/dt)$  can be respectively replaced in Eq. 13a by  $H$ , the steady state dispersion height, and  $Q/A$ , the volume flow rate per unit area of the dispersion, to give

$$\frac{H}{Q/A} = \frac{1}{k_1} + \frac{1}{k_2} H \quad (13b)$$

A similar equation was derived by Stönnner and Wöhler (1975) by analogy with a two-stage successive chemical reaction. Equations 13a and 13b can be written explicitly in the reciprocal forms

$$\frac{1}{-dh/dt} = \frac{1}{k_1} \frac{1}{h} + \frac{1}{k_2} \quad (14a)$$

and

$$\frac{1}{Q/A} = \frac{1}{k_1} \frac{1}{H} + \frac{1}{k_2} \quad (14b)$$

The value of  $Q/A$  can of course be replaced by  $Q_d/A\epsilon_F$ , where  $Q_d$  is the dispersed phase flow rate and  $\epsilon_F = Q_d/Q = R/(1+R)$  is the feed hold-up when  $R$  is the dispersed to the continuous phase flow rate ratio.

In Eq. 13a,  $h/(-dh/dt)$  can be considered as the notional residence time of the batch dispersion which, when plotted with respect to  $h$ , would yield a straight line with intercept  $1/k_1$  and slope  $1/k_2$ . Thus, the values of  $k_1$  and  $k_2$  can be obtained from batch settling data. Alternatively, Eq. 14a can be integrated with the initial condition  $h = h_0$  when  $t = 0$  to give

$$t = \frac{1}{k_1} \ln \left( \frac{h_0}{h} \right) + \frac{1}{k_2} (h_0 - h) \quad (15)$$

from which  $k_1$  and  $k_2$  can be calculated from the experimental decay of  $h$  with  $t$ .

The values of  $k_1$  and  $k_2$  so obtained from either Eq. 13a, 14a, or 15 can be used in Eq. 13b or 14b to predict the variation of  $H$  with  $Q/A$ . This implies that the range of  $-dh/dt$  encountered in the batch experiments should correspond to the range of dispersion flux  $Q/A$  for which the steady state dispersion heights are to be predicted. This can only be so if the drop sizes, dispersed phase hold-up, and degree of turbulence are similar in the batch and continuous experiments. So the unsteady state conditions should be chosen to match those at the steady state.

#### Application

The data of Vieler (1977) have been used to test the model. The conditions for their six steady state experiments are listed in Table

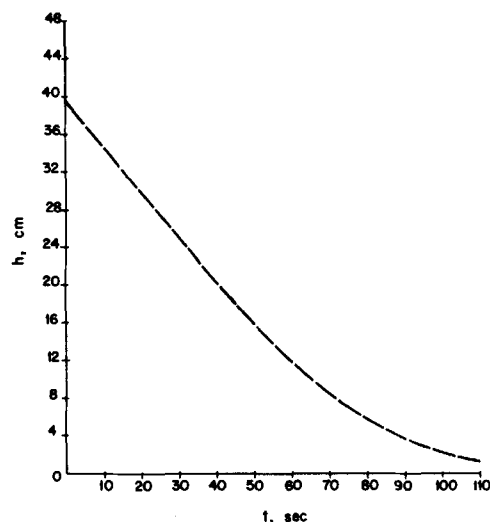


Figure 4a. Variation of batch dispersion height  $h$  with time  $t$  for the batch run corresponding to continuous run 4; data of Vieler (1977).

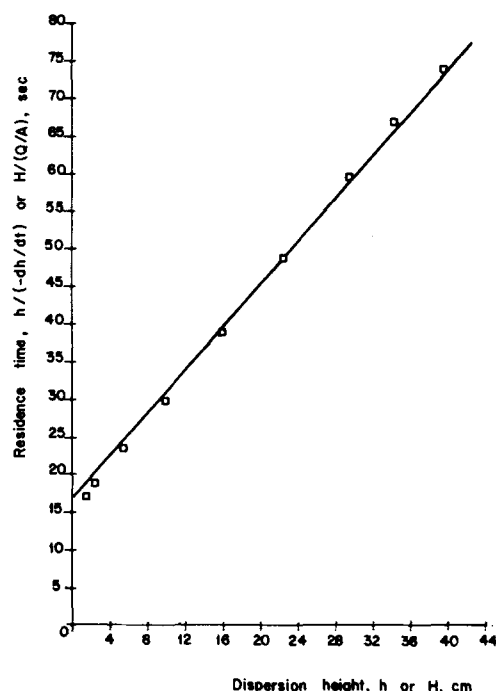


Figure 4b. Variation of steady state height  $H$  with dispersion residence time  $H/(Q/A)$  for continuous run 4 (solid line) compared with variation of batch height  $h$  with notional residence time  $h/(-dh/dt)$  for corresponding batch run (open squares); data of Vieler (1977). Slope of line =  $1/k_2$ ; intercept on residence time axis =  $1/k_1$ .

1. More than 20 batch tests with different initial heights were performed for each of the continuous runs. Using Eq. 15 we have computed the values of  $k_1$  and  $k_2$  from least square fits for each of their batch experiments. These are then used to calculate the steady state dispersion height  $H$  from Eq. 13b, which is then compared with the experimental steady state dispersion height reported by Vieler et al. The agreement between the experimentally obtained steady state dispersion height and that predicted from the batch results is found to be very good for those batch settling experiments having the same range of dispersion flux as in the steady state experiments when similar conditions exist. The batch variation of  $h$  with  $t$  corresponding to continuous run 4 is shown in Figure 4a and the relationship between the batch and continuous residence times  $h/(-dh/dt)$  and  $H/(Q/A)$  with the dispersion heights  $h$  and  $H$ , respectively, is confirmed in Figure 4b. For the batch data the intercept on the ordinate axis gives  $1/k_1 = 15.2$  s and the slope of

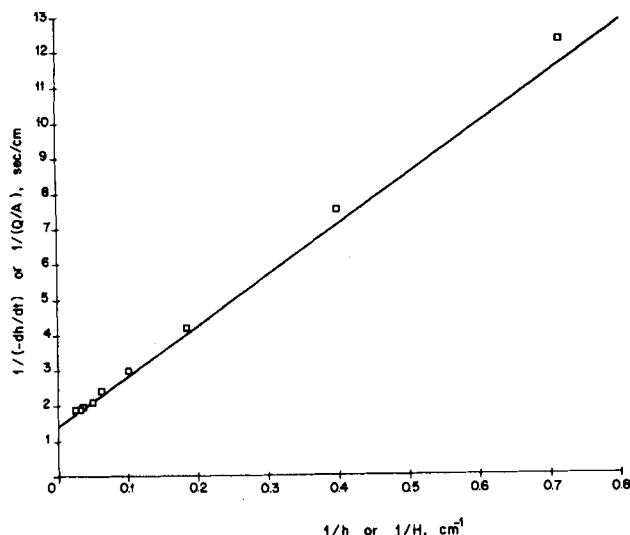


Figure 4c. Variation of reciprocal throughput  $1/(Q/A)$  with reciprocal steady state height  $1/H$  for continuous run 4 (solid line) compared with variation of  $1/(-dh/dt)$  with reciprocal batch height  $1/h$  for corresponding batch run (open squares); data of Vieler (1977). Slope of line =  $1/k_1$ ; Intercept on the ordinate =  $1/k_2$ .

the line  $1/k_2 = 1.49$ . The reciprocal relationship is shown in Figure 4c, from which the same values of  $1/k_1$  and  $1/k_2$  are obtained from the slope and intercept, respectively.

The ranges of  $Q/A$  and  $-dh/dt$  are also found to be approximately the same for the continuous runs 5 and 6 and their corresponding batch experiments. Figure 5a gives typical batch settling curves with different initial heights corresponding to the steady state run 6. The comparison between the experimental steady state dispersion heights and those predicted from the corresponding batch settling data is shown in Figure 5b. The points refer to the variation of  $H$  with  $Q/A$  predicted from the batch settling curves having the same range of dispersion flux at the interface as that in the steady state runs while the solid line corresponds to the experimental variation of  $H$  with  $Q/A$ . Good agreement is also obtained between the continuous runs 4 and 5 and the variations predicted from the corresponding batch experiments. The average error between the experimental and predicted steady state dispersion heights is only 11% for each of the runs 4, 5, and 6. This is at least as good as would be obtained from expensive pilot plant experiments and must be considered more than acceptable in an industrial context.

#### Sigmoidal Batch Decay

As explained in the Introduction, this type of curve occurs when the initial rates of drop sedimentation and coalescence are slow. However, if the rate of sedimentation is higher than the rate of coalescence of drops with their homophase, a dense-packed layer is formed adjacent to the disengaging interface. The batch dispersion height  $h$  is the sum of the sedimentation and dense-packed heights  $h_s$  and  $h_p$  in which the average holdups are  $\bar{\epsilon}_s$  and  $\bar{\epsilon}_p$ . However, in practice it is the heights  $x$  and  $y$  of the sedimenting and coalescing interfaces relative to the final undisturbed interface which are measured. So  $h_s$  and  $h_p$  must be predicted from the sedimentation and coalescence rates  $-dx/dt$  and  $-dy/dt$ , respectively. These possess maximum values which occur at the inflection points in the variation of  $x$  and  $y$  with time  $t$ .

#### Sedimentation Height

The batch decay data of Barnea and Mizrahi (1975d) for the phase system A at 29°C [water-in-oil (w/o) dispersion  $\bar{\epsilon}_o = 0.5$ ] is shown in Figure 7. For the sedimentation of drops in a dense-packed dispersion the general relationship between the settling velocity  $V_s$  and drop diameter  $\phi$  is

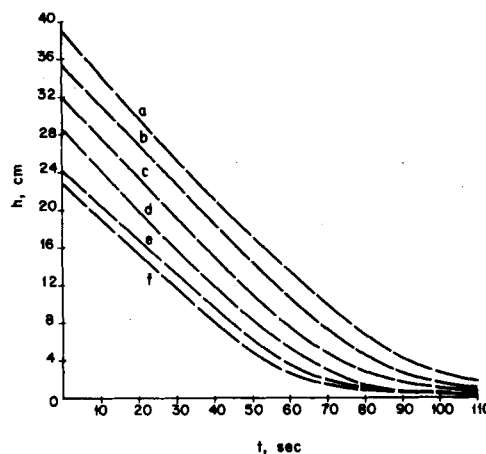


Figure 5a. Variation of batch dispersion height  $h$  with time  $t$  for runs a, b, c, d, e, and f, corresponding to continuous run 6; data of Vieler (1977).

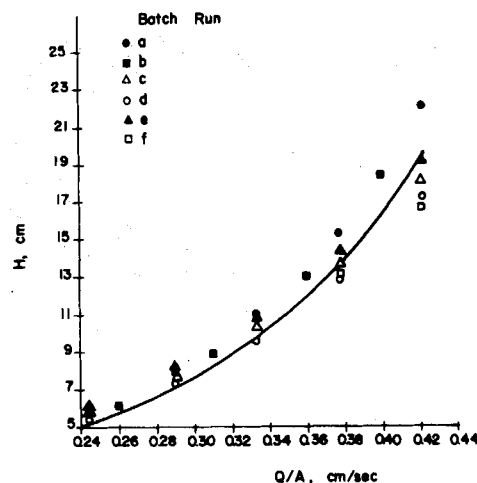


Figure 5b. Variation of steady state dispersion height  $H$  with throughput  $Q/A$  for continuous run 6 (line) compared with variation predicted by batch runs a, b, c, d, e, and f.

$$V_s = K_s \phi^r \quad (16)$$

where  $K_s$  is a function of the physical properties and dispersed phase holdup fraction  $\bar{\epsilon}_s$ . For laminar flow Barnea and Mizrahi (1975e) found experimentally that  $r = 2$ , which corresponds to Stokes' law for single drops when  $K_s = \Delta\rho g/18\mu_c$ . For turbulent flow, Kumar et al. (1980) found  $r = 1/2$ , for the intermediate flow regime  $2 > r > 1/2$ , changing only slowly as the Reynolds number,  $\rho_c V_s \phi / \mu_c$ , increases. Assuming that the dispersed phase holdup in the sedimentation zone  $\bar{\epsilon}_s$  is constant and that the drop diameter grows with time according to Eq. 6b, gives

$$-\frac{dx}{dt} = k_s t^{r/n} \quad (17)$$

where  $-dx/dt$  is the settling velocity  $V_s$  of the drops relative to the continuous phase, and  $k_s = K_s \phi_o^n (n/6\tau_{bo})^{r/n}$ . Integrating with the initial condition  $x = x_o$  when  $t = 0$  yields

$$x_o - x = \frac{k_s}{1 + r/n} t^{1+r/n} \quad (18)$$

A plot of  $\ln(x_o - x)$  vs.  $\ln t$  up to the inflection point thus yields the index  $r/n$  and constant  $k_s$ . The batch decay data of Barnea and Mizrahi (1975d) for their phase system A at 29°C (w/o dispersion,  $\bar{\epsilon}_o = 0.5$ ) plotted in Figure 6 indicates that  $k_s = 0.054$  and  $r/n = 0.42$ . The sedimentation equation can then be written as

$$-\frac{dx}{dt} = 0.054 t^{0.42} \quad (19)$$

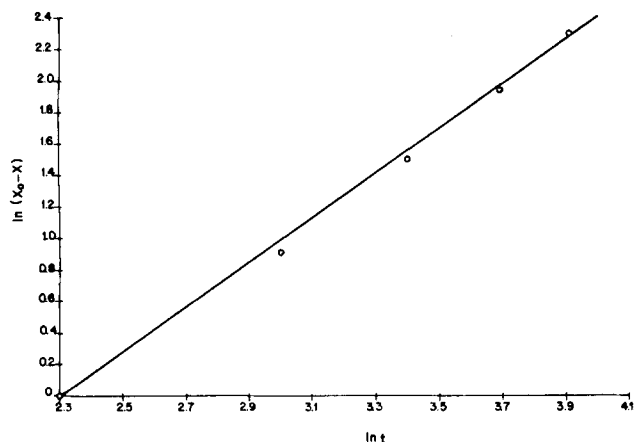


Figure 6. Variation of  $\ln(x_o - x)$  with  $\ln t$  for the sedimentation front up to inflection point for phase system A, w/o dispersion ( $\bar{\epsilon}_o = 0.5$ ) at 29°C; Barnea and Mizrahi (1975d).

where  $-dx/dt$  is the drop velocity relative to the stagnant continuous phase in the batch settling experiments. For continuous settler the equivalent drop velocity is  $Q_d/A\bar{\epsilon}_s$  and the residence time of drops in the sedimentation zone is  $t = \bar{\epsilon}_s H_s A / Q_d$ , so the analog of Eq. 19 becomes:

$$\frac{1}{\bar{\epsilon}_s} \frac{Q_d}{A} = 0.054 \left( \frac{\bar{\epsilon}_s H_s A}{Q_d} \right)^{0.42} \quad (20)$$

which can be rewritten as

$$H_s = 1043 \frac{1}{(\bar{\epsilon}_s)^{3.4}} \left( \frac{Q_d}{A} \right)^{3.4} \quad (21)$$

#### Thickness of Dense-Packed Layer

A decaying batch dispersion consists of a sedimenting zone of height  $h_s$  and a dense-packed zone of height  $h_p$ , so that the total dispersion height  $h$  at any time  $t$  is

$$h_s + h_p = h \quad (22)$$

If the instantaneous average dispersed phase holdup fractions in these zones are  $\bar{\epsilon}_s$  and  $\bar{\epsilon}_p$  respectively, then a volume balance for

the dispersed phase at any time  $t$  gives

$$\bar{\epsilon}_s h_s + \bar{\epsilon}_p h_p = \bar{\epsilon} h \quad (23)$$

where  $\bar{\epsilon}$  is the instantaneous average holdup fraction of the dispersed phase for the entire dispersion. At any time  $t$ , the volume of coalesced dispersed phase is proportional to  $(y_o - y)$  and the volume of clear continuous phase to  $(x_o - x)$ . It follows that the volumes of dispersed and continuous phases in the dispersion are proportional to  $y$  and  $x$  and the dispersed phase holdup  $\bar{\epsilon} = y/(x + y)$ , so that

$$\bar{\epsilon}_s h_s + \bar{\epsilon}_p h_p = y \quad (24)$$

where

$$x + y = h \quad (25)$$

In a decaying dispersion the boundary between the sedimentation and dense-packed zones is often hazy, making  $h_s$  and  $h_p$  difficult to determine. It is more convenient to measure  $x$  and  $y$ , the heights of the sedimenting and coalescing interfaces relative to the final undisturbed interface. Eliminating  $h_s$  from Eqs. 22 and 24 yields

$$h_p = \frac{(y - \bar{\epsilon}_s h)}{(\bar{\epsilon}_p - \bar{\epsilon}_s)} \quad (26)$$

so the locus  $z = y - h_p$  of the boundary between the sedimentation and dense-packed zones is:

$$z = \frac{\bar{\epsilon}_s x - y(1 - \bar{\epsilon}_p)}{(\bar{\epsilon}_p - \bar{\epsilon}_s)} \quad (27)$$

The maximum value of  $h_p$  occurs when

$$\bar{\epsilon}_s = (-dy/dt)/(-dh/dt) \quad (28)$$

which coincides with the inflection point in the variation of  $y$  with  $t$  if the gradients are measured at the point which we will designate by  $y_{inf}$ ,  $t_{inf}$ . The initial value of  $h_p$  is then given by

$$h_{po} = \frac{(y_o - \bar{\epsilon}_s h_o)}{(\bar{\epsilon}_p - \bar{\epsilon}_s)} \quad (29)$$

So if  $h_p$  is to be zero when  $t = 0$ , Eq. 26 has to be rewritten in the form

$$h_p - h_{po} = \frac{(y - \bar{\epsilon}_s h)}{(\bar{\epsilon}_p - \bar{\epsilon}_s)} \quad (30)$$

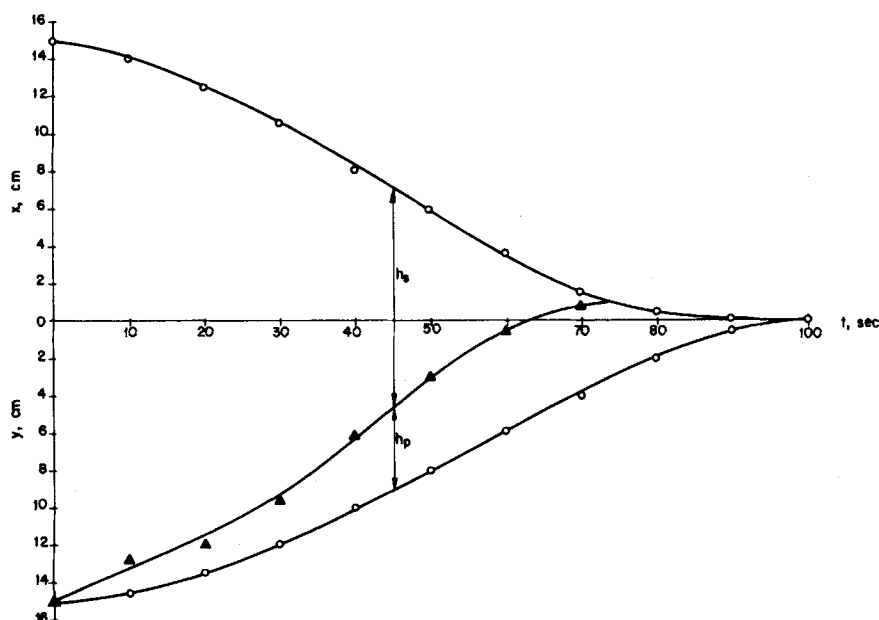


Figure 7. Variation of sedimenting and coalescing heights  $x$  and  $y$  measured relative to final undisturbed interface with time  $t$  for the Phase System A. (Also shown: locus of interface between sedimentation and dense-packed zones with heights  $h_s$  and  $h_p$  for  $\bar{\epsilon}_s = 0.5$  and  $\bar{\epsilon}_p = 0.75$ .)

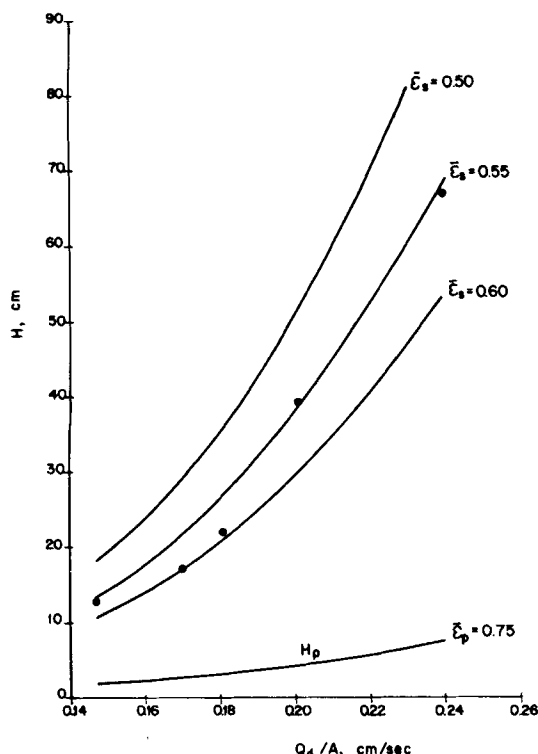


Figure 8. Experimental variation of steady state height  $H$  with dispersed phase throughput  $Q_d/A$  compared with sum of sedimentation and dense-packed heights  $H_s$  and  $H_p$  predicted by Eqs. 21 and 34 for  $\bar{\epsilon}_s = 0.50, 0.55$ , and  $0.60$ . Locus of  $H_p$  for  $\bar{\epsilon}_p = 0.75$  is shown separately.

where  $\bar{\epsilon}_s$  is given by Eq. 28 in which both gradients are measured at  $y_{inf}$ ,  $t_{inf}$ . Should  $\bar{\epsilon}_s$  equal the initial hold-up  $\bar{\epsilon}_0 = y_o/h_o$  then  $h_{po} = 0$  and  $h_p$  and  $z$  are given by

$$h_p = \frac{(y h_o - y_o h)}{(\bar{\epsilon}_p h_o - y_o)} \quad (31)$$

and

$$z = \frac{y_o x - y h_o (1 - \bar{\epsilon}_p)}{(\bar{\epsilon}_p h_o - y_o)} \quad (32)$$

#### Application

Figure 7 shows the variation in  $h_p$  predicted by Eq. 31 with  $\bar{\epsilon}_p = 0.75$  for phase system A (w/o dispersion at 29°C, with  $\bar{\epsilon}_0 = 0.5$ ) of the data of Barnea and Mizrahi (1975d). Corresponding values of  $-dy/dt$  are obtained from a polynomial fit of  $y$  with  $t$  and can be correlated with  $\bar{\epsilon}_p h_p$  by the following equation to within an error of  $\pm 6.2\%$ :

$$\bar{\epsilon}_p h_p = 355 \left( -\frac{dy}{dt} \right)^{2.91} \quad (33)$$

Since  $-dy/dt$  is the volume rate of coalescence per unit area, the corresponding steady state equation for a continuous settler is

$$\bar{\epsilon}_p H_p = 355 \left( \frac{Q_d}{A} \right)^{2.91} \quad (34)$$

The steady state dispersion height  $H$  can then be found by adding the values of  $H_s$  and  $H_p$  from Eqs. 21 and 34, respectively. The value of  $\bar{\epsilon}_s$  for the steady state dispersion may of course differ from that during batch decay because of different turbulence conditions and drop growth rates. Furthermore, it is clear from Eq. 21 that  $H_s$  is sensitive to small variations in  $\bar{\epsilon}_s$ . Figure 8 compares the values of  $H$  predicted for three values of  $\bar{\epsilon}_s$ , together with the values of  $H$  measured experimentally as a function of  $Q_d/A$ . It can be seen that agreement between the predicted and experimentally obtained steady state dispersion heights is good when  $\bar{\epsilon}_s$  lies between 0.55 and 0.6.

#### Empirical Correlations

Barnea and Mizrahi (1975d) correlated the nominal settler capacity  $Q/A$ , corresponding to an arbitrary steady state dispersion height of  $H$  of 50 cm, to the batch separation time  $t_f$  for a batch dispersion of an initial height of 30 cm. For phase system A (w/o dispersion) they obtained:

$$\left( \frac{Q}{A} \right) = 888 t_f^{-0.9} \quad (35)$$

However, even if  $t_f$  is known, only the throughput corresponding to a steady state dispersion height of 50 cm can be calculated from this equation. In fact, their data for phase system A (both w/o and o/w dispersions) can be extended to all steady state heights by correlating the experimental values of  $H$ ,  $Q/A$ , and  $t_f$ . For each steady state height a linear relationship between  $t_f$  and  $t_r$  (the residence time of the continuous dispersion  $HA/Q$ ) exists:

$$t_r = m t_f + c \quad (36)$$

Table 2 gives the values of  $m$ ,  $c$ , and the percentage deviation between the experimental and calculated  $t_r$  for both types of dispersion obtained from a least squares fit. Since both  $m$  and  $c$  vary with  $H$ , further linear relationships:

$$m = m_h H + c_h \quad (37)$$

and

$$c = m_c H + c_c \quad (38)$$

are obtained, the slopes  $m_h$ ,  $m_c$ , and intercepts  $c_h$  and  $c_c$  being listed in Table 3.

Equation 36 written in the reciprocal form thus becomes:

$$H = \frac{(1/k_1) \frac{Q}{A}}{1 - (1/k_2) \frac{Q}{A}} \quad (39)$$

in which  $1/k_1 = c_h t_f + c_c$  and  $1/k_2 = m_h t_f + m_c$ , where  $1/k_1$  and  $1/k_2$  have units of seconds and s/cm respectively. Equation 39 thus enables  $H$  (in cm) to be calculated for a given value of dispersion throughput  $Q/A$  (in cm/s) from a single experimental measurement of the batch separation time  $t_f$  (in s) for an initial batch dispersion height of 30 cm. For both w/o and o/w dispersions this equation predicts  $H$  to within  $\pm 20\%$  for 90% of the data presented by Barnea and Mizrahi (1975d) for their phase system A. This is

TABLE 2.  $m$  and  $c$  VALUES OF  $t_r = m t_f + c$  FOR PHASE SYSTEM A OF BARNEA AND MIZRAHI (1975d) FOR DIFFERENT STEADY STATE DISPERSION HEIGHTS

$H$ cm	$m$		$c, s$		% Deviation* on $t_r$	
	Water/Oil Dispersion	Oil/Water Dispersion	Water/Oil Dispersion	Oil/Water Dispersion	Water/Oil Dispersion	Oil/Water Dispersion
20	0.5535	0.5541	8.84	1.5135	13.9	12.8
40	0.9868	0.8396	9.35	6.871	14.9	12.8
60	1.3690	1.0155	10.37	19.50	15.4	14.6

\* 90% of data points have only 10% deviation.



TABLE 3.  $m_h$ ,  $c_h$  AND  $m_c$ ,  $c_c$  VALUES OF EQS. 37 AND 38 FOR PHASE SYSTEM A OF BARNEA AND MIZRAHI (1975d)

Dispersion	$m = m_h H + c_h$			$c = m_c H + c_c$		
	$m_h$ cm <sup>-1</sup>	$c_h$	% Deviation on $m$	$m_c$ s/cm	$c_c$ s	% Deviation on $c$
Water/Oil	0.0204	0.1543	1.7	0.03825	8.0	1.9
Oil/Water	0.01154	0.3415	4.4	0.4497	-8.7	35.0

considerably worse than the accuracy obtained from the physical models based on exponential and sigmoidal batch decay curves. In any case, the results apply only to the system used by Barnea and Mizrahi (1975d) and can only be extended to other systems by performing extensive pilot plant experiments in addition to unsteady-state batch experiments.

## CONCLUSIONS

1. The steady state height  $H$  in a continuous settler is related to the dispersion throughput  $Q/A$  by the reciprocal equation

$$\frac{1}{Q/A} = \frac{1}{k_1} \frac{1}{H} + \frac{1}{k_2} \quad (\text{I})$$

which indicates that flooding will occur when  $Q/A = k_2$ . Below the flooding point the relationship between  $H$  and the dispersed phase flow rate  $Q_d/A$  is often expressed by

$$H = K(Q_d/A)^w \quad (\text{II})$$

in which  $Q_d = \epsilon_F Q$  where  $\epsilon_F = R/(1 + R)$  is the dispersed phase hold-up fraction in the feed and  $R = Q_d/Q_c$ , the flow ratio of the dispersed to continuous phases; the index  $w$  is invariably greater than 2, even when  $Q_d/A$  is replaced by  $Q/A$ . Relationships could be clouded by trace amounts of surface active material which make reproducible results very difficult to obtain.

2. The height  $h$  of a batch dispersion either decays exponentially with time or passes through inflection point. In the latter case the rates of sedimentation and coalescence of drops with their homophase initially increase and then decrease. So the variation in heights  $x$  and  $y$  of the sedimenting and coalescing interfaces are also sigmoidal. The volume sedimentation rate  $-\bar{\epsilon}_s dx/dt$  is invariably higher than the coalescence rate  $-dy/dt$  of drops with their homophase. So a dense-packed layer of height  $h_p$  and mean hold-up  $\bar{\epsilon}_p$  is formed adjacent to the disengaging interface. The total dispersion height  $h = x + y = h_s + h_p$ , where  $h_s$  is the height of the sedimentation zone in which the mean holdup is  $\bar{\epsilon}_s$ .

3. Equation I can be obtained by assuming that the total throughput  $Q/A$  depends on the thickness of the dense-packed zone which may be expressed as a function of the dispersion height. The analogous equation for the batch decay is

$$\frac{1}{-dh/dt} = \frac{1}{k_1} \frac{1}{h} + \frac{1}{k_2} \quad (\text{III})$$

which can be readily integrated to give  $h$  as a function of time  $t$ . Values of  $1/k_1$  and  $1/k_2$  obtained from either of these batch equations can be employed in Eq. I to predict the variation in steady state height with dispersion throughput if the drop size, hold-up, turbulence, dispersion flux, and of course the degree of contamination, are similar in both batch and continuous experiments.

4. Allowing for drop growth by binary coalescence, the variation in batch sedimentation rate  $-dx/dt$  with time  $t$  is given in cgs units by:

$$-dx/dt = 0.054 t^{0.42} \quad (\text{IV})$$

The sedimenting drops collect to form a dense-packed layer of height  $h_p$ , so the force per unit area of the disengaging interface due to the weight of the drops is proportional to  $\bar{\epsilon}_p h_p$ . This determines the volume rate of coalescence of the drops with their homophase  $-dy/dt$  through the equation:

$$\bar{\epsilon}_p h_p = 355 (-dy/dt)^{2.9} \quad (\text{V})$$

5. In Eq. IV the sedimentation rate  $-dx/dt$  can be replaced at the steady state by the drop velocity  $Q_d/A\bar{\epsilon}_s$ . Similarly, the elapsed time  $t$  can be replaced by the drop residence time in the sedimentation zone,  $H_s A \bar{\epsilon}_s / Q_d$ . So the steady state equivalent of Eq. IV is

$$H_s = 1,043 (Q_d/A\bar{\epsilon}_s)^{3.4} \quad (\text{VI})$$

In Eq. V the dense-packed height  $h_p$  and volume rate of coalescence  $-dy/dt$  are directly equivalent to  $H_p$  and  $Q_d/A$  respectively. So the steady state equation becomes

$$\bar{\epsilon}_p H_p = 355 (Q_d/A)^{2.9} \quad (\text{VII})$$

Adding  $H_s$  and  $H_p$  gives the steady state dispersion height  $H$  if the hold-ups  $\bar{\epsilon}_s$  and  $\bar{\epsilon}_p$  in the batch and continuous experiments respectively may be equated, which is only possible when the turbulence conditions are similar. Equations VI and VII can be approximated by a single power function in the form of Eq. II with a corresponding loss in accuracy.

6. Other authors have empirically related the batch separation time  $t_f$  corresponding to a standardized initial height  $h_o$  to the dispersion throughput  $Q/A$ , producing a given steady state height  $H$ . Generalization of this relationship, using the experimental data of Barnea and Mizrahi (1975d), leads to Eq. I, in which  $1/k_1$  and  $1/k_2$  are known linear functions of  $t_f$ . However, the empirical constants involved are functions of the phase system and operating conditions employed. The effort needed to redetermine these constants for other systems and conditions is extensive.

7. It is much simpler and more accurate to use the models described above which relate the batch decay and steady state behavior of dispersions through Eqs. I and III or IV, V, VI, and VII. Providing that the physical properties of the liquid systems and the range of operating conditions including the coalescence flux used in the small-scale batch experiments are similar to those in the large-scale continuous settler, it is possible to predict the steady state dispersion height as a function of throughput from unsteady-state decay data. The small scale batch experiments are much easier to carry out than costly pilot plant experiments. These models have been verified with available experimental data on industrial systems and should greatly simplify the future design and scale-up of mixer-settlers.

## NOTATION

$A$	= cross-sectional area of batch or continuous settler
$g$	= acceleration due to gravity
$h$	= height of dispersion in batch settler
$H$	= height of dispersion in continuous settler
$k_1, k_2, k_s, K_s$	= constants
$\ln$	= natural logarithm
$m$	= exponent on drop size during coalescence at disengaging interface
$n$	= exponent on drop size during growth due to binary coalescence
$N$	= number of drops in a given volume of dispersion
$p, q$	= indices in function $f(ch/\epsilon_* h_*)$
$Q/A$	= sum of volume flow rates of dispersed and continuous phases per unit area in a continuous settler
$Q_d/A$	= volume flow rate per unit area of dispersed phase in a continuous settler

$t$	= time
$t_f$	= final batch separation time
$t_r$	= residence time of dispersion
$V_s$	= relative velocity between drops and continuous phase
$x$	= distance of sedimenting interface from final undisturbed interface in batch dispersion
$y$	= distance of coalescing (disengaging) interface from final undisturbed interface in batch dispersion

#### Greek Letters

$\gamma_i$	= shape factor
$\epsilon$	= holdup fraction of dispersed phase in dispersion
$\epsilon_F$	= holdup in feed of continuous settler
$\bar{\epsilon}$	= average holdup
$\bar{\epsilon}_p$	= average holdup in dense-packed zone
$\bar{\epsilon}_s$	= average holdup in sedimentation zone
$\mu_c$	= continuous phase viscosity
$\Delta\rho$	= density difference between continuous and dispersed phases
$\tau_b$	= binary coalescence time
$\tau_i$	= coalescence time of drops at coalescing interface
$\phi$	= drop diameter in dispersion
$\phi_i$	= drop diameter at coalescing interface
$\psi_i$	= volume rate of coalescence per unit area

#### Subscripts

*	= reference condition
$i$	= coalescing interface
$F$	= feed to steady state settler
$o$	= initial condition
$p$	= dense-packed layer
$s$	= sedimentation zone

#### LITERATURE CITED

- Barnea, E., and J. Mizrahi, "Separation Mechanism of Liquid/Liquid Dispersions in a Deep-Layer Gravity Settler. I: The Structure of the Dispersion Band," *Trans. Inst. Chem. Engrs.*, **53**, 61 (1975a).  
 ———, "Separation Mechanism of Liquid/Liquid Dispersions in a Deep-Layer Gravity Settler. II: Flow Patterns of the Dispersed and Continuous Phases within the Dispersion Band," *Trans. Inst. Chem. Engrs.*, **53**, 70 (1975b).  
 ———, "Separation Mechanism of Liquid/Liquid Dispersions in a Deep-Layer Gravity Settler. III: Hindered Settling and Drop-to-Drop Coalescence in the Dispersion Band," *Trans. Inst. Chem. Engrs.*, **53**, 75 (1975c).  
 ———, "Separation Mechanism of Liquid/Liquid Dispersions in a Deep-Layer Gravity Settler. IV: Continuous Settler Characteristics," *Trans. Inst. Chem. Engrs.*, **53**, 83 (1975d).  
 ———, "A Generalized Approach to the Fluid Dynamics of Particulate Systems. 2: Sedimentation and Fluidisation of Clouds of Spherical Liquid Drops," *Can. J. Chem. Eng.*, **53**, 461 (1975e).  
 Burrill, K. A., and D. R. Woods, "Film Shapes for Deformable Drops at Liquid/Liquid Interfaces. III: Drop Rest Times," *J. Colloid Interface Sci.*, **42**, 35 (1973).  
 Charles, G. E., and S. G. Mason, "The Coalescence of a Liquid Drop with Flat Liquid/Liquid Interfaces," *J. Colloid Sci.*, **15**, 236 (1960).  
 Davies, G. A., G. V. Jeffreys, and D. V. Smith, "Coalescence of Liquid Droplets—Correlation of Coalescence Times," *Proc. Int. Sol. Extr. Conf.*, **1**, 385 (1971).  
 Godfrey, J. C., et al., "The Interpretation of Batch Separation Tests for Liquid/Liquid Mixer-Settler Design," *Proc. Int. Sol. Extr. Conf.* 1977, Can. Inst. of Mining & Metallurgy, **1**, 406 (1979).  
 Golob, J., and R. Modic, "Coalescence of Liquid/Liquid Dispersions in Gravity Settlers," *Trans. Inst. Chem. Engrs.*, **55**, 207 (1977).  
 Hanson, C., and A. H. Brown, "Secondary Droplet Formation During Drop Coalescence," *Inst. Chem. Engrs. Symp. Ser.*, **26**, 57 (1967).  
 Jeffreys, G. V., and J. L. Hawksley, "Coalescence of Liquid Droplets in Two-Component Two-Phase Systems. I: Effect of Physical Properties on the Rate of Coalescence," *AIChE J.*, **11**, 413 (1965).  
 Komazawa, I., and T. Otake, "Stabilities of a Single Drop at a Liquid/Liquid Interface and of Multi-Drops in a Drop-Layer," *J. Chem. Eng., Japan*, **3**, 243 (1970).  
 Kumar, A., D. K. Vohra, and S. Hartland, "Sedimentation of Droplet Dispersions in Counter-Current Spray Columns," *Can. J. Chem. Eng.*, **58**, 154 (1980).  
 Lawson, G. B., "Coalescence Processes," *Chem. Process Eng.*, **48**(5), 45 (1967).  
 Ryon, A. D., F. L. Daley, and R. S. Lowrie, "Scale-up of Mixer-Settlers," *Chem. Eng. Prog.*, **55**(10), 70 (1959).  
 Ryon, A. D., F. L. Daley, and R. S. Lowrie, "Design and Scale-Up of Mixer-Settlers for a Dapex Solvent Extraction Process," Report No. ORNL-2951, Oak Ridge Natl. Lab., Tennessee (1960).  
 Ryon, A. D., and R. S. Lowrie, "Experimental Basis for the Design of Mixer-Settlers for the Amex Solvent Extraction Process," Report No. ORNL-3381, Oak Ridge Natl. Lab., Tennessee (1963).  
 Stöner, H. M., and F. Wöhler, "An Engineer's Approach to a Solvent Extraction Problem," *Inst. Chem. Engrs. Symp. Ser.*, **42**, 14.1 (1975).  
 Vieler, A. M. S., "A Model for the Design of Deep-Layer Gravity Settlers from Batch Data," M.Sc. Dissertation, Univ. Witwatersrand, Johannesburg, South Africa (1977).  
 Vieler, A. M. S., D. Glasser, and A. W. Bryson, "The Relationship between Batch and Continuous Phase-Disengagement," *Proc. Int. Sol. Extr. Conf.*, 1977, Can. Inst. of Mining & Metallurgy, **1**, 399 (1979).

Manuscript received Dec. 5, 1983; revision received Mar. 28, 1984; and accepted Apr. 1.